Journal of Asian Earth Sciences 254 (2023) 105755

Contents lists available at ScienceDirect

Journal of Asian Earth Sciences

journal homepage: www.elsevier.com/locate/jseaes

Detrital zircon U-Pb dating of Late Mesozoic strata in the Junggar Basin, NW China: Implications for the timing of collision between the Karakoram-Lhasa Block and the Eurasian continent

Zhaojian Wu [a], Xiaoyong Yang [b,*], Saijun Sun [c,*], Jiang Zhu [d], Xiaowen Hu [b], Xiaozhong Han [a], Yifeng Cai [e], Hui Ji [a]

[a] China Coal Geology Group Corporation Limited, Beijing 100040, China
[b] CAS Key Laboratory of Crust-Mantle Materials and Environments, University of Science and Technology of China, Hefei 230026, China
[c] Center of Deep Sea Research, Institute of Oceanology, Center for Ocean Mega-Science, Chinese Academy of Sciences, Qingdao 266071, China
[d] School of Earth Sciences, Yunnan University, Kunming 650500, China
[e] Institute of Geophysics, Petroleum Exploration and Development Institute of Xinjiang Oilfield Company, Urumqi 830011, China

ARTICLE INFO

Keywords:
Detrital zircon U-Pb dating
Intraplate deformation
Junggar Basin
Karakoram-South Pamir collision
Lhasa-Qiangtang collision

ABSTRACT

As a sensitive marker of plate collision events, intraplate compressional deformation can be used to provide a unique regional perspective for the contemporaneous complicated tectonic evolution at the plate margin. Two regional intraplate deformation and uplift events of the late Middle Jurassic and Late Jurassic-Early Cretaceous in the Junggar Basin were revealed through seismic interpretation and geological profiles, and both of them correspond to unconformity in the sedimentary successions. Detrital zircons from Jurassic and Cretaceous strata in the eastern margin of Junggar Basin were selected for LA-ICP MS U-Pb dating. Combined with previous detrital zircon U-Pb dating data, a prominent, time-continuous group of syn-depositional detrital zircons has been discovered in the Jurassic-Cretaceous strata of the Junggar basin, and their discontinuous distribution in the strata above and below the unconformity restricts the precise timing of the corresponding regional intraplate deformation to ca.166–157 Ma and ca.151–129 Ma, respectively, which coincide well with tectono-magmatic events in southern Tibet. Based on previous apatite fission track dating data in Sayan-Siberia orogenic belt and Tianshan-Beishan orogenic belt, we suggest that stages of regional intracontinental deformation in the Junggar Basin and its periphery are related to compressive events on the southern margin of Eurasia. Among them, the first stage of intraplate deformation during ca. 166–157 Ma with shorter duration and slighter intensity may be controlled by the collision of the Karakoram-Lhasa Block with the South Pamir Block and the second during ca.151–129 Ma with longer duration and more intensity may signify the main process of Lhasa and Qiangtang collision and the final full closure of the Bangong-Nujiang Tethys Ocean.

1. Introduction

There is increasing recognition that compressional intraplate deformation at or near the Earth's surface may occur well away from plate boundaries (Hendrix et al., 1992; Neil and Houseman, 1997; Marshak et al., 2000; Cloetingh and Van Wees, 2005; Cunningham, 2005; Buslov et al., 2007; Aitken et al., 2009; Jolivet et al., 2010; Glorie et al., 2011; Parizot et al., 2020; Stephenson et al., 2020) and it is highly sensitive and can be acted as a marker to tectonic events at plate boundaries (Parizot et al., 2020). That's because, in the absence of mantle vertical forces and local plate-margin interactions, tectonic evolution in the interior of continents is controlled by far-field horizontal compressive stresses at plate boundaries, with the lithosphere playing an effective role in stress guidance (Ziegler et al., 1998; Bosworth et al., 1999; Raimondo et al., 2014; Pinet, 2016).

After the closure of the Tian Shan Ocean and Junggar Ocean in Late Carboniferous- Early Permian (Chen et al., 1999; Li et al., 2015; Zhang et al., 2015, 2016; Liu et al., 2017; Han and Zhao, 2018; Xu et al., 2021), the Junggar Block began the journey of inland evolution, forming a prominent field laboratory for the study of compressional intraplate deformation and far-field effects (Yang et al., 2015; Morin et al., 2018; Fang et al., 2019; He et al., 2022). Although stratigraphic contact

* Corresponding authors.
E-mail addresses: xyyang@ustc.edu.cn (X. Yang), sunsaijun06@163.com (S. Sun).

https://doi.org/10.1016/j.jseaes.2023.105755
Received 30 March 2023; Received in revised form 30 May 2023; Accepted 8 June 2023
Available online 14 June 2023

relationship can roughly constrain the age of tectonic events recorded in the strata, for example, the extensively developed T/J unconformity in the Junggar Basin is proposed to be associated with the Qiangtang collision (Hendrix et al., 1992; Dumitru et al., 2001; Yang et al., 2015), many of Mid-Late Jurassic and Early Cretaceous deformation currently appear to be inconsistent with the tectonic events in the Eurasian margin. The main reason is that the precise sedimentary ages of the strata themselves are not well defined, which hinders the determination of the deformation timing recorded in the strata and the further understanding of the relationship between intraplate deformation and the far-field effect of plate edge stress.

In this paper, detrital zircon ages offer the possibility to constrain the precise timing of tectonic events recorded in sedimentary rocks, and the occurrence time of Mesozoic unconformities in the Junggar Basin offers a new perspective to better understand the tectonic evolution of the Eurasian margin in a regional context.

2. Geological setting and unconformities in Late Mesozoic

Junggar Block is a compressional triangle zone due to the convergence of the Siberian Plate, Kazakhstan Plate, and Tarim Plate in the Mesozoic (Fig. 1a). The Mesozoic and Cenozoic Altai-Sayan orogeny to the northeast of the Junggar Basin is often considered to be related to the Mongolia-Okhotsk tectonic system (De Grave et al., 2009, 2014; Vetrov et al., 2016), while Meso-Cenozoic deformation in the Tian Shan orogenic belts to the south of the Junggar Basin is proposed to be the product of the collisions in South Asia (Hendrix et al., 1992; Dumitru et al., 2001; De Grave et al., 2011; Glorie et al., 2019). Therefore, the Junggar Basin is often regarded as the transitional site of these two tectonic systems, and its inland tectonic evolution is closely related to them. According to the Paleozoic distribution pattern of depression and uplift and the Meso-Cenozoic tectonic reworking, the basin is divided into six secondary tectonic units, and the structural styles and stratigraphic distribution characteristics of different units are quite different (Fig. 1b). However, from the whole basin, the Jurassic-Cretaceous inland sediments in different units can be considered as an approximately identical complete tectonic-sedimentary cycle, and the records of stratigraphic unconformity can help us better understand the basin-range coupling in the late Mesozoic.

Several unconformities were discovered in the Mesozoic strata of the Junggar Basin through seismic interpretation. The truncation surface between the Jurassic and Lower Cretaceous is visible throughout the basin(Fig. 1c-1f), suggesting strong uplift and denudation in the Latest Jurassic-Earliest Cretaceous. The interface between the Xishanyan

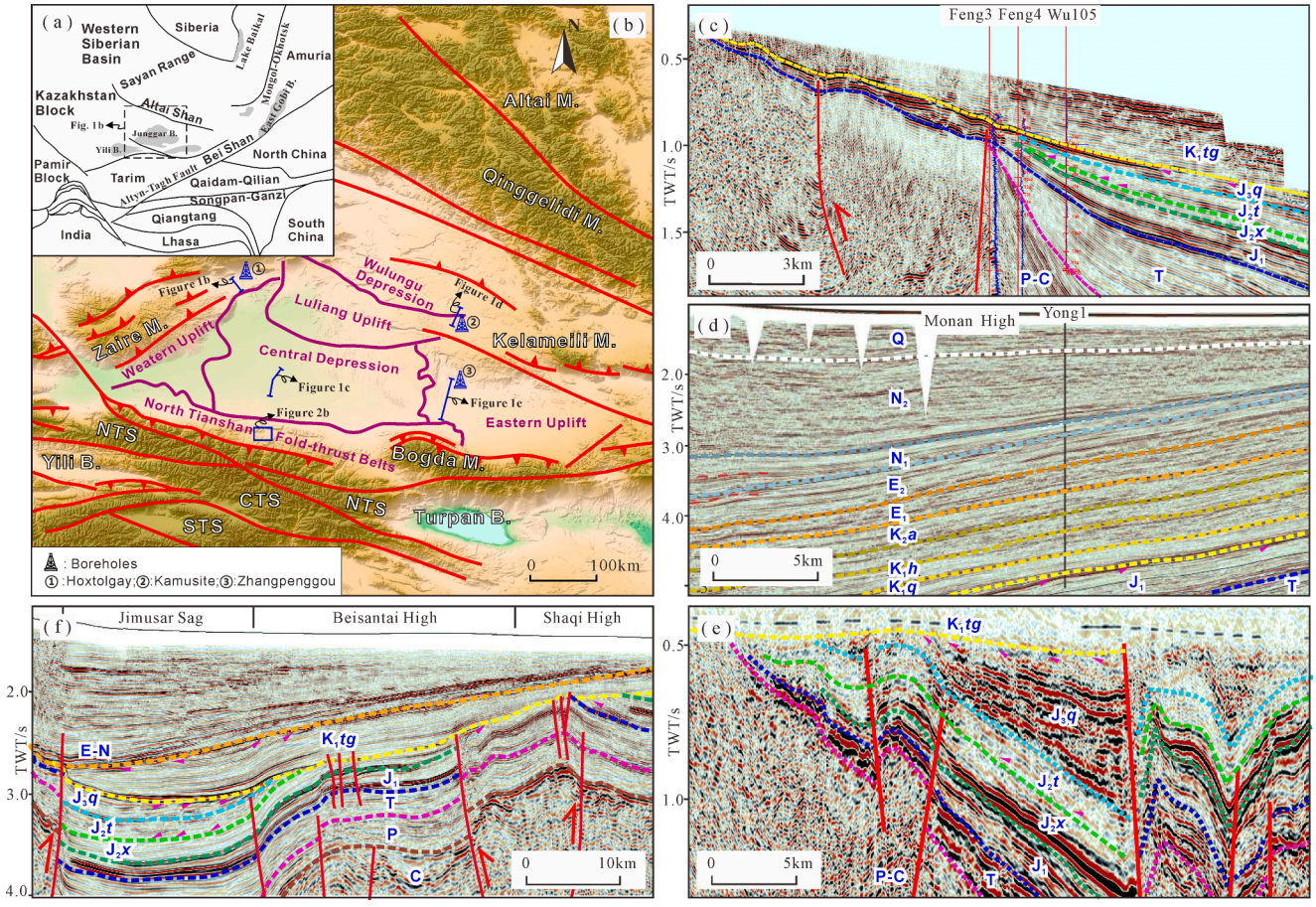

Fig. 1. (a) Schematic tectonic map of Asia and location of the Junggar Basin. (b) Topographic and tectonic map of the Junggar basin and adjacent areas (DEM, GEBCO_2022 grid). (c) Interpreted seismic profile in the Western Uplift. The bottom boundary of the Toutunhe Formation corresponds to an onlap, and the boundaries of the Badaowan Formation and Tugulu Group correspond to truncation. (d) Interpreted seismic profile in the Central Depression, after Zhang, 2020. The boundary between the Upper Cretaceous and Paleocene is conformity contact in the Southern Junggar Basin and that between the Lower Cretaceous and Jurassic is a truncated unconformity. (e) Seismic interpretation of WL9427 profile in the northeastern Junggar Basin. The bottom interface of the Lower Cretaceous is a truncated unconformity surface, that of the Toutunhe Formation is onlap, and the properties of the J/T interface are unknown. (f) Part of seismic profile 2019-SN07 in the eastern Junggar Basin. The bottom of the Toutunhe Formation corresponds to an onlap, and those of the Tugulu Group and Paleogene are truncations. The original seismic profiles of Fig. 2(c), 2(e), and 2(f) are provided by Xinjiang Oilfield Company of PetroChina. The abbreviations are NTS = North Tian Shan; CTS = Central Tian Shan; STS = South Tian Shan; M = Mountain; B = Basin. Purple solid triangles indicate the termination of seismic reflection. (For interpretation of the references to colour in this figure legend, the reader is referred to the web version of this article.)

Formation and the Toutunhe Formation shows a typical feature of onlap in the northwestern and northeastern margin of the basin(Fig. 1c and 1e), and progradation in the southern margin(Fig. 1f), indicating a depositional discontinuity after Xishanyao period.

The observation of the outcrop or drilling core shows that Xishanyao Formation is dominated by delta plain subfacies at the basin margin and is thought to be the main coal measure strata in the area (Fig. 2a and 2f). The typical braided river sediments developed in the Toutunhe period, with the erosion surface at the bottom contacting with the underlayer (Fig. 2c and 2f). The Tugulu Group is a shallow lake-flood plain deposit in an arid environment, and its contact relationship with the underlying strata can not be well constrained in the drilling core (Fig. 2g). In addition, although the Lower Cretaceous Tugulu Group was truncated and in unconformable contact with the Paleogene in the northwestern Junggar Basin and its peripheral Hoxtolgay Basin (Fig. 2a), the Upper Cretaceous is in conformable contact with the Paleogene in the southern margin of the basin(Fig. 2e).

3. Detrital zircon U-Pb dating and age distribution in the Junggar Basin

3.1. Sampling and analytical methods

Detrital zircons were obtained from Jurassic and Cretaceous sandstones in the Kamusite area of the northeastern Junggar Basin and locations and lithology of samples are shown in Fig. 2 and Supplementary Table S1. Zircon separation was completed at Xinhang Surveying and Mapping Institute, Langfang, Hebei Province. Refined zircon samples were extracted by flotation and magnetic separation methods, embedded onto epoxy mounts manually, polished to expose the interior and gilded. Cathode-luminescence (CL) was photographed at the Institute of Geology and Geophysics, Chinese Academy of Sciences to reveal the internal structure of zircons. LA-ICP-MS U-Pb isotopic dating of zircon was performed using an Agilent 7900 inductively coupled plasma mass spectrometer attached to GeoLasPro 193 nm ArF excimer laser

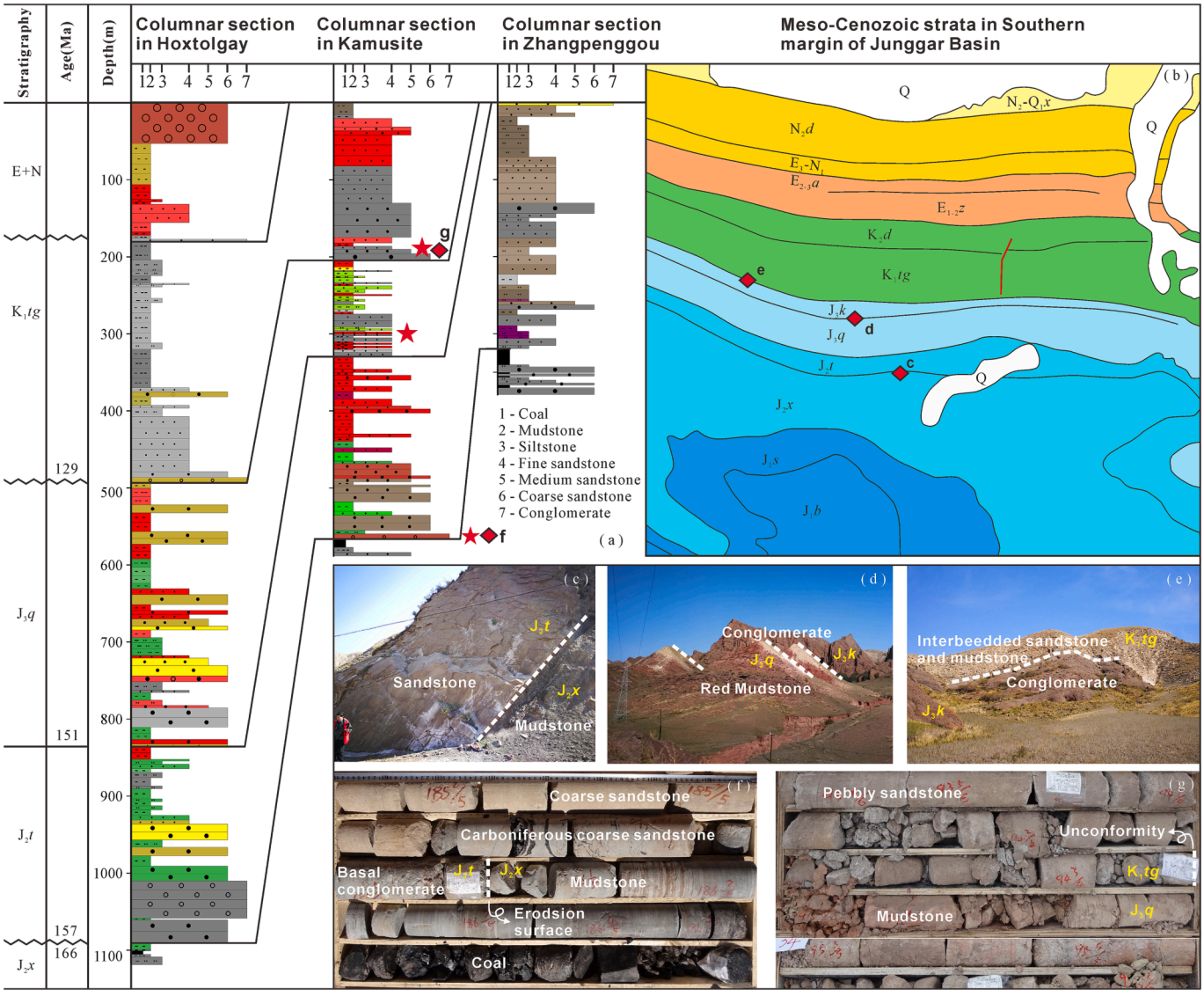

Fig. 2. Correlation of stratigraphy, lithology, and typical photographs of main late Mesozoic stratigraphic units of the Junggar Basin. The lithology and typical photographs are from our field and well observations and two unconformities of J_2x/J_2t and J_3/K_1tg can be identified clearly. The sedimentation ages of the Tugulu Group, Qigu Formation, and Toutunhe Formation come from this study and are different from previous studies such as Yang et al. (2015, 2017). Red diamonds represent field observation points in the southern margin of the Junggar Basin, and five-pointed stars mean the main sampling strata. The stratigraphic codes are J_1b = Badaowan Formation; J_1s = Sangonghe Formation; J_2x = Xishanyao Formation; J_2t = Toutunhe Formation; J_3q = Qigu Formation; J_3k = Kalaza Formation; K_1tg = Tugulu Group; K_2d = Donggou Formation; $E_{1-2}z$ = Ziniquanzi Formation; $E_{2-3}a$ = Anjihaihe Formation; N_2d = Dushanzi Formation. (For interpretation of the references to colour in this figure legend, the reader is referred to the web version of this article.)

ablation system at the Key Laboratory of Mineral Resources Evaluation in Northeast Asia, Ministry of Natural Resources, Jilin University, Changchun, China. Helium was used as the carrier gas of the ablative material. Zircons 91500 (Wiedenbeck et al., 1995) were used as external standards and NIST610 as monitoring standards. Detrital zircons with obvious cracks or inclusions were excluded, and grains of various sizes and shapes were randomly selected to ensure that each age component is statistically representative. The GLITTER software was used for the calculation of U-Pb isotope ratios and element contents, and the common-Pb correction was performed following the method in Andersen (2002). A detailed analytical procedure is shown by Yuan et al. (2004).

3.2. Age distribution of detrital zircons

Detrital zircons in sandstones show dominantly well-developed oscillatory zoning or sector zoning (Fig. 3) and their Th/U ratios are prevailingly >0.4 and therefore a register of igneous crystallization (Hartmann and Santos, 2004; Wu and Zheng, 2004). Zircon Th/U ratios and U-Pb ages of individual data processing are shown in Supplementary Table S2, and zircon isotope data collected from previous studies are provided in Supplementary Table S3. Zircon U-Pb Concordia diagrams of some samples are shown in Fig. 4a-4e. The method used for visualizing detrital age distributions in this paper is the Kernel Density Estimation (KDE) and the software package is the Java-based DensityPlotter program developed by Vermeesch (2012). The age distribution of late Mesozoic detrital zircons in the northeastern and southern Junggar Basin is similar and different. Both of them range from Archean to Early Cretaceous, with three principal components of ca. 180–130 Ma (P1), ca. 280–350 Ma (P2), and ca. 400–480 Ma (P3), as well as some sporadic distributions larger than 600 Ma (Fig. 4f-4 g). Among them, the most conspicuous Component P1 is missing from the provenance but contemporaneous with the stratigraphic deposition, indicating that these zircons are syn-sedimentary detrital grains. Moreover, these syn-depositional detrital zircons are time-continuous and approximately normally distributed, and the later the deposition of strata, the younger the kernel density of Component P1 (Fig. 5).

4. Discussion

4.1. Provenance of detrital zircon populations in the Junggar Basin

Although no coeval igneous rocks of Component P1 have been reported in possible provenance areas except for a few tuff intercalations (Wang and Gao, 2012; Wang et al., 2022), the detrital age components P2 and P3 of strata from Xishanyao Formation to Tugulu Group correspond well to the age distributions of igneous zircons in Kalamaili Mountain (Fig. 4h). A small number of ca.275 Ma detrital zircons were found in the Xishanyao Formation and the Toutunhe Formation, which may be related to the uplift and denudation of the Qinggelidi Mountain during ca.160 Ma (Fig. 4i; Li, 2007). While an important observation is that the distinctive ca. 375 Ma age peak of zircons in Qinggelidi Moutain is rather weak in samples from the northeastern Junggar basin. Likewise, the ca.440 Ma detrital zircon ages are essentially absent in zircons from Qinggelidi Moutain. All these observations strongly confirm the interpretation that the Kalamaili Mountain is the main and constant provenance of the Jurassic and Lower Cretaceous in the eastern Junggar basin, and Qinggelidi Mountain may provide a low proportion of provenance for the Xishanyao Formation and the Toutunhe Formation.

Similarly, magmatic rocks corresponding to Component P1 of detrital ages are also rarely reported in the Chinese Tian Shan (Liu et al., 2019a), in spite that Fang et al. 2015a speculated that they were the product of large-scale volcanic activity. By contrast, the Carboniferous continental arc rocks and post-collision back-arc rocks in North Tian Shan are often considered as the source rocks of Component P2 (Fig. 4j; Dong et al., 2011; Chen et al., 2013; Zhang et al., 2015, 2016; Long et al.,

Fig. 3. Typical cathode luminescence images of detrital zircons from Mesozoic strata in the Kamusite area. Detrital zircons with obvious cracks or inclusions were excluded, and grains of various sizes and shapes were randomly selected.

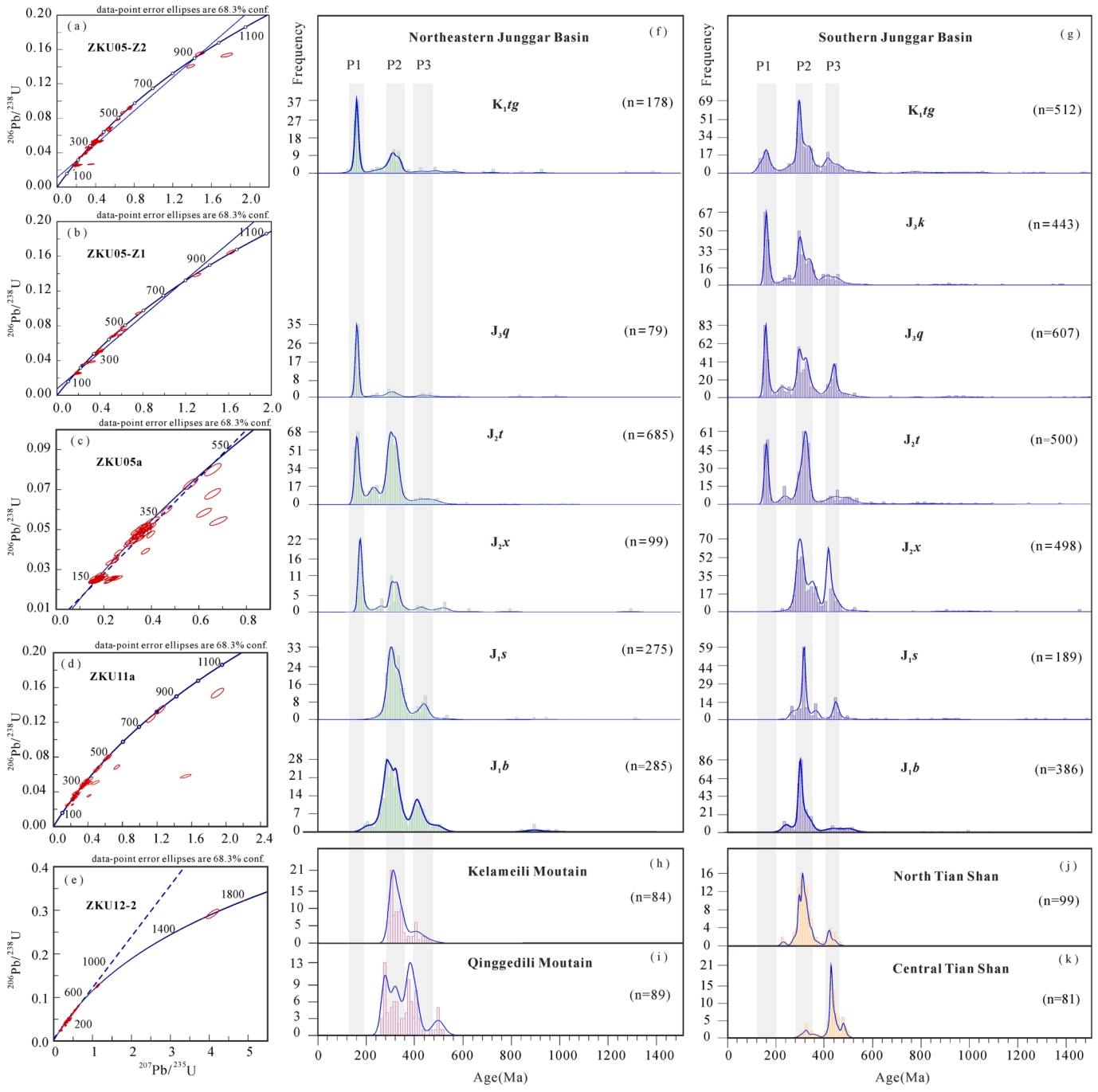

Fig. 4. Zircon U–Pb concordia diagrams and age distribution. (a-e) Detrital zircon U–Pb concordia diagrams of sandstones in the northeastern Junggar Basin; (f-g) Age distribution of detrital Zircon from late Mesozoic strata in the northeastern and southern margins of the Junggar Basin; (h-k) Age distribution of magmatic zircons in the peripheral orogenic belt of the basin. Since the Middle Jurassic, syn-depositional detrital zircons have emerged in the Junggar Basin with a conspicuous and time-continuous age composition of ca. 180–130 Ma and contemporaneous magmatic rocks are scarce in the basin periphery. Comparison of age distributions of detrital and magmatic zircons suggests that the Kalamaili Mountain is the main and constant provenance of the Jurassic and Lower Cretaceous in the eastern Junggar basin, and the North Tian Shan is the continuous, stable, and major provenance of the southern margin of the Junggar Basin.

2020), while the Ordovician-Early Devonian subduction-related island arc rocks in Central Tian Shan as that of Component P3 (Fig. 4k; Charvet et al., 2011; Dong et al., 2011; Fang et al., 2015a; Zhu et al., 2021). These correlations suggest that the North Tian Shan is a continuous, stable, and major provenance of the southern margin of the Junggar Basin and that the Central Tian Shan also provided a partial provenance during the Jurassic and Early Cretaceous. In summary, the provenance of Jurassic and Cretaceous is stable in both the eastern and southern Junggar Basin.

4.2. *Timing of intraplate deformation of the Junggar Basin*

In the case of constant provenance, which has been corroborated above, the chronologically continuous distribution of syn-depositional detrital zircon ages (Component P1) makes it possible to constrain the timing of stratigraphic deposition, depositional discontinuities, and intraplate deformation of the Junggar Basin.

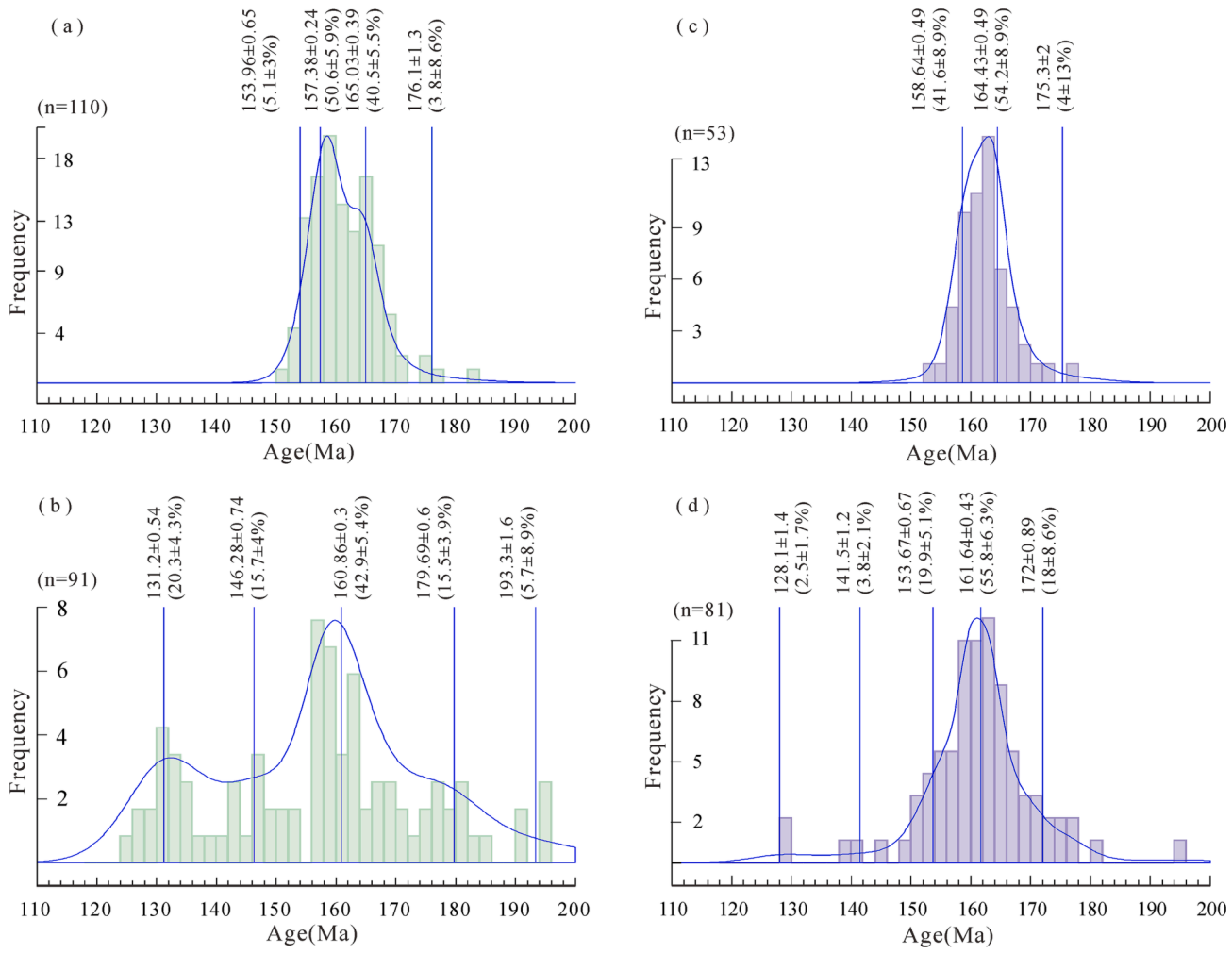

Fig. 5. Kernel density estimation of Component P1 of late Mesozoic detrital zircons. (a) KDE of Component P1 of Toutunhe Formation in the Southern Junggar Basin; (b) KDE of Component P1 of Tugulu Group in the Southern Junggar Basin; (c) KDE of Component P1 of Toutunhe Formation in the Eastern Junggar Basin; (d) KDE of Component P1 of Tugulu Group in the Eastern Junggar Basin. The Tugulu Group has a smaller KDE of Component P1 than the Toutunhe Formation in both the southern and eastern Junggar Basin.

4.2.1. Timing of intraplate deformation in late Middle Jurassic

The unconformity between Xishanyao Formation and Toutunhe Formation means that the Junggar Basin suffered intraplate deformation after the deposition of the Xishanyao Formation and before that of the Toutunhe Formation, and the exact age of deformation can be constrained by the maximum depositional age (MDA). The maximum likelihood age (MLA) model of Galbraith and Laslett (1993) and Galbraith (2005) and the R package named IsoplotR (Vermeesch, 2018) are proposed to adopt in MDA estimation (Vermeesch, 2021).

In the northeastern Junggar Basin, the MDA of the Xishanyao Formation is 166.00 ± 2.03 Ma (Supplementary Table S3 and Fig. 6a) after removing sample KT-05-75 with a low concordance degree, and that of the Toutunhe Formation is 159.52 ± 0.86 Ma (Supplementary Table S3 and Fig. 6b). Since the provenance did not change, a large amount of grains ranging from 166 to160Ma in the Toutunhe Formation and Tugulu Group is absent in the Xishanyao Formation, indicating that the Xishanyao Formation should have been deposited before 166 Ma. As a result, the precise timing of depositional discontinuity, or intraplate deformation, between the Xishanyao Formation and Toutunhe Formation in the northeastern Junggar Basin can be constrained to ca.166–160 Ma.

Compared with the northeastern Junggar Basin, the most significant difference in the distribution of detrital zircons in the southern Junggar Basin is that no Component P1 has been found in the Xishanyao Formation (Fig. 4). The MDA of the Toutunhe Formation in the southern margin was estimated to be 156.99 ± 0.45 Ma (Fig. 6c), and the Kernel Density Estimation (KDE) of Component P1 features a first major peak at 165.03 ± 0.39 Ma (40.5 ± 5.5%) and a second mode at 157.38 ± 0.24 Ma (50.6 ± 5.9%) (Fig. 5c). Since the late Mesozoic provenance in the southern margin of the Junggar Basin did not change significantly, we conclude that the only reason that a large number of detrital zircons belonging to the P1 Component from the Toutunhe Formation, such as 165–157 Ma, are not present in the Xishanyao Formation is that the Xishanyao Formation was deposited before ca.165 Ma. This would underscore the inference that the precise timing of intraplate deformation between the Xishanyao Formation and Toutunhe Formation in the southern margin of the Junggar Basin is ca.166–157 Ma. In summary, the late Middle Jurassic intraplate deformation of the Junggar Basin occurred during 166–157 Ma.

4.2.2. Timing of intraplate deformation in Latest Jurassic to Earliest Cretaceous

The unconformity between the Upper Jurassic Qigu or Kalaza formation and the Lower Cretaceous Tugulu Group is widespread throughout the Junggar Basin. Although the MDA of ZKU05-Z1 at the bottom of the Qigu Formation in the northeastern Junggar Basin was 160.68 ± 0.68 Ma(Fig. 6d), 19 clastic particles younger than MDA could be found, with a minimum age of 152.72 ± 1.87 Ma(Supplementary

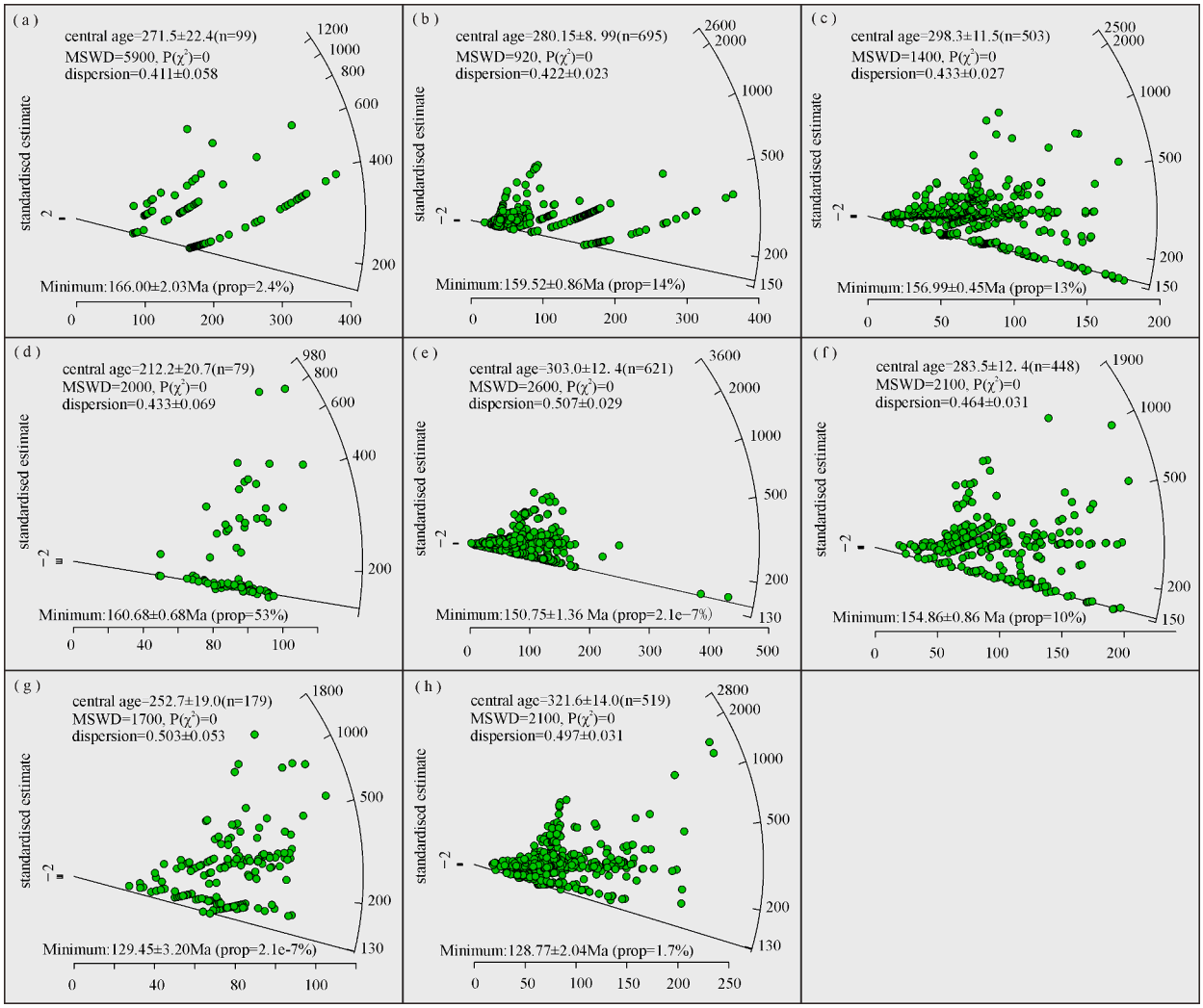

Fig. 6. Radial plots of maximum depositional age (MDA) of Late Mesozoic strata can be used to restrict the precise intraplate deformation timing corresponding to the late Middle Jurassic unconformity to ca.166–157 Ma, and the timing corresponding to the Latest Jurassic-Earliest Cretaceous unconformity to 151–129 Ma in the Junggar Basin. (a) The MDA of the Xishanyao Formation in the northeastern Junggar Basin is 166.0 ± 2.03 Ma. (b) The MDA of the Toutunhe Formation in the northeastern Junggar Basin is 159.52 ± 0.86 Ma. (c) The MDA of the Toutunhe Formation in the southern margin of the Junggar Basin is 156.99 ± 0.45 Ma. (d) The MDA of the Qigu Formation in the northeastern Junggar Basin was 160.68 ± 0.68 Ma. (e)The MDA of the Qigu Formation in the southern Junggar Basin was 150.75 ± 1.36 Ma. (f) The MDA of the Kalazha Formation in the southern Junggar Basin was 154.86 ± 0.86 Ma. (g) the MDA of samples from Tugulu Group was 129.45 ± 3.20 Ma. (h) the MDA of the Tugulu Group in the southern margin of Junggar Basin was estimated to be 128.77 ± 2.04 Ma. Since a large amount of grains ranging from 166 to 160 Ma in the Toutunhe Formation and Tugulu Group is absent in the Xishanyao Formation, indicating that the Xishanyao Formation should have been deposited before 166 Ma. Therefore, the precise time of depositional discontinuity between the Xishanyao Formation and Toutunhe Formation in the Junggar Basin can be constrained to 166–157 Ma. Similarly, those clastic grains smaller than 151 Ma, which are absent in the Upper Jurassic but prevalent in the overlying Tugulu Group, indicates that the Upper Jurassic should have been deposited before 151 Ma. It means that the Tugulu Group should be deposited after ca.129 Ma. Thus, the precise timing of Late Jurassic-Early Cretaceous unconformity or intraplate deformation can be limited to ca.151–129 Ma.

Table S3). The MDA of the Qigu Formation(J_3q) and Kalazha Formation (J_3k) in the southern margin of the Junggar Basin was 150.75 ± 1.36 Ma and 154.86 ± 0.86 Ma, respectively (Supplementary Table S3; Fig. 6e-6f). Similarly, those clastic grains smaller than 151 Ma, which are absent in the Upper Jurassic but prevalent in the overlying Tugulu Group, indicates that the Upper Jurassic should have been deposited before 151 Ma.

In the northeastern Junggar Basin, the MDA of samples from the Tugulu Group was 129.45 ± 3.20 Ma (Fig. 6g), accompanied by a large number of 130–135 Ma clastic grains in the same strata (Zhu et al., 2021; Wang, 2009; Yang, 2012). Meanwhile, the MDA of the Tugulu Group in the southern margin of the Junggar Basin was estimated to be 128.77 ± 2.04 Ma through published detrital zircon ages(Fig. 6h). It means that the Tugulu Group should be deposited after ca.129 Ma, that is, unconformity or intraplate deformation occurred before ca.129 Ma. Thus, the precise timing of Late Jurassic-Early Cretaceous unconformity or intraplate deformation can be limited to ca.151–129 Ma.

4.3. *Plausible driving force of intraplate deformation of the Junggar Basin*

A series of global studies on the correlation between intraplate deformation and plate boundary collision demonstrated the high sensitivity of the former to the latter, and intraplate deformation is commenced when full collisional plate coupling was achieved and subduction ceased (Bosworth et al., 1999; Dickerson, 2003; Pinet, 2016; Stephenson et al., 2020; Parizot et al., 2020). Ziegler et al. (1998) reviewed several scenarios related to intraplate deformation and proposed that the most likely to propagate compressional stresses to the interior of a continent is the collisional interaction at plate boundaries (Ziegler et al.,1998; Roberts and Houseman, 2001; Raimondo et al.,

2014). Accordingly, the late Mesozoic intraplate deformation of the Junggar Basin is considered to be the product of tectonic activity in the Eurasian continental margin, which may be related to the closure of Mongolia-Okhotsk Ocean (MO) or Bangong-Nujiang Ocean (BNO) and the far-field effect of their corresponding orogeny (Graham et al., 2001; De Grave and Buslov, 2007; Ma et al., 2015). Previously published apatite fission track (AFT) dating data and representative cooling models from the Siberian Altai-Sayan and Tian Shan were collected and compared (Fig. 7 and Supplementary Table S4). The Siberian Altai-Sayan experienced a tectonic quiescence throughout the Jurassic with most of the cooling and AFT ages being in Late Cretaceous. Whereas the Tianshan experienced two phases of accelerated cooling of ca. 200–190 Ma and 165–150 Ma in the Jurassic and two periods of ca.120–100 Ma and 90–80 Ma in the Cretaceous with AFT ages ranging from 200 to 0 Ma. More likely, the closure of MO exerted extensive intraplate deformation in Siberian Altai-Sayan and shaped its current topography, but the impact on the Tianshan is uncertain. (Graham et al., 2001; De Grave and Van den haute, 2002; De Grave et al., 2009, 2014; Ma et al.,2015; Glorie and De Grave, 2016). Therefore, this would underscore the interpretation that those two periods of intraplate deformation mentioned above are related to the collision along the southern margin of Eurasia and its far-distant effect.

4.4. Constraints on the tectonic evolution of the southern margin of Eurasia

4.4.1. Controversy over tectonic events on the southern margin of Eurasia

The complex tectonic evolution of the southern margin of Eurasia in the Late Mesozoic is still puzzling. Among them, The Lhasa-Qiangtang collision is considered to be the most important tectonic event and the occurrence time remains hotly controversial with three mainstream hypotheses:

Hypothesis I postulates that the initiation of the Lhasa-Qiangtang collision occurred in the late Bathonian (ca.166 Ma). The Mesozoic stratigraphic unconformity record and provenance differences in the Bangong-Nujiang suture zone (BNSZ) are interpreted as the development of the arc-trench system and initiation of the Lhasa-Qiangtang collision in ca. 166 Ma (Ma et al.,2017; Sun et al.,2019). However, opponents argue that the subduction and subsequent retardation of the ocean plateau or microcontinent on the BNO could also have caused deformation in the southern Qiangtang Basin (Chen et al., 2018; Yan and Zhang, 2020; Shi et al., 2020).

Hypothesis II insists The collision occurred during the latest Jurassic to earliest Cretaceous (ca.150–130 Ma). The sedimentary, stratigraphic, and paleomagnetic results from Lhasa and Qiangtang blocks demonstrate the Lhasa-Qiangtang collision initial at the late Jurassic (Leier et al., 2007; Zhu et al., 2016; Bian et al., 2017; Li et al., 2017, 2019; Zhao et al., 2017; Ma et al., 2018; Chen et al., 2020; Wei et al., 2020; Wang et al., 2022; Zeng and Sun, 2022), and the magmatic gap between 145 and 130 Ma on the southern Qiangtang terrane result from the termination of normal subduction (Zhu et al., 2016; Li et al., 2020; Chen et al., 2020). Unsurprisingly, the opposition is overwhelming. Observations such as forearc MORB-like and OIB-type mafic rocks at 138–134 Ma (Zeng et al., 2021) and magmatic assemblages with arc-affinities at ca. 110–104 Ma (Hao et al., 2019) strongly refute the southern Qiangtang being transformed into a non-marine environment in Lastest Jurassic to Earliest Cretaceous and promote the magmatic gap being the result of flat subduction of an oceanic plateau.

Hypothesis III suggests that the collision terminated in the early Late Cretaceous (ca.100–90 Ma). The coexistence of enormous Mid-Cretaceous MORB-like, OIB-type mafic rocks, and marine sedimentary rocks along the BNSZ, accompanying a magmatic arc of ca.110–90 Ma in the southern Qiangtang terrane, indicates the Lhasa-Qiangtang collision did not occur until the Late Cretaceous (Chen et al., 2018; Liu et al., 2018; Shi et al., 2020; Yang et al., 2022). Nevertheless, the stratigraphic records of the northern Lhasa terrane, as well as paleomagnetic data, show that it was already welded to the southern margin of Eurasia at ca.122–100 Ma (Ma et al., 2018; Lai et al., 2019; Li et al.,2020; Wu

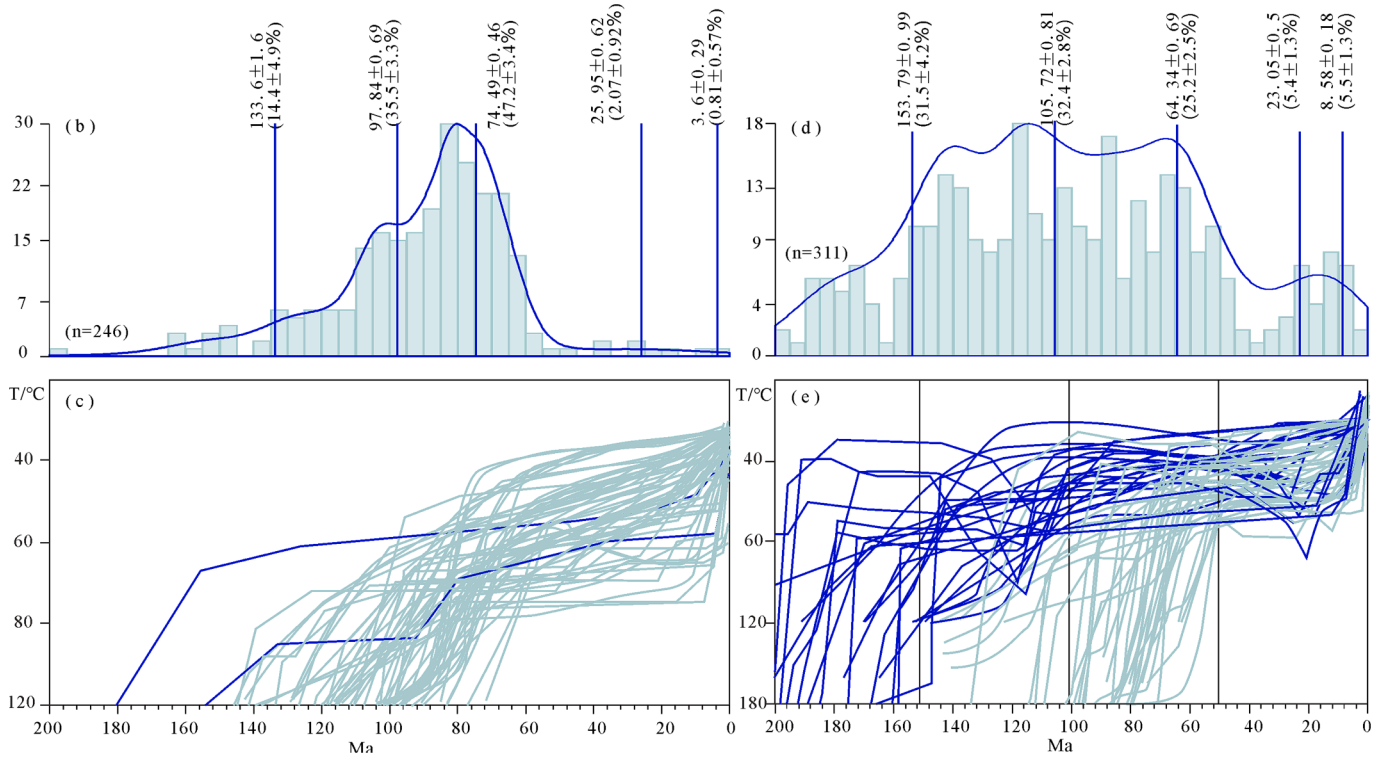

Fig. 7. Comparison of AFT age distribution and cooling curves of the Siberian Altai-Sayan and Tian Shan. The AFT ages of Altai-Sayan, adjacent to the northeastern Junggar Basin, are mostly less than 110 Ma with a peak of ca. 90–80 Ma(a and b), while the AFT age of Chinese Tianshan, Southwest Tianshan, and areas located to the south of the Junggar Basin are extensively distributed between ca.170–60 Ma(c and d).

et al.,2022; Zhu et al., 2022), which is consistent with high-Mg adakitic magmatism younger than 100 Ma in central Tibet (Sun et al., 2015; Yi et al.,2018; Liu et al., 2019b; Sun et al., 2020; Luo et al., 2021).

In addition, debates on the timing of the Karakoram-South Pamir collision also vary greatly. Sedimentary records of the northern Karakoram Block and subduction-related magmatism in the southwestern Pamir were used to demonstrate the collision occurred before the Middle Jurassic (Gaetani et al, 1993, 1996; Zanchi and Gaetani, 2011; Gaetani et al, 2013). While, on the observation of the stratigraphic contact relationship, sedimentary facies types, and magmatic rock distribution of Karakoram and Pamir plates, Yang et al. (2015, 2017) proposed that the Karakoram and Lhasa blocks were a single giant block and the western Karakoram-Lhasa Block initially collided with the South Pamir Block during Callovian (probably started at ca.167 Ma), resulting in deformation and exhumation in northwest China and Kyrgyzstan.

4.4.2. *Insight from intraplate deformation of the Junggar Basin*

The lack of clarity about how many times and when these collisions occurred on the southern margin of Eurasia may be the main cause of these disputes. Complicated geological processes often obscure the truth. Therefore, it may be more beneficial to understand the tectonic events solely concerning the propagation of compressive stress to the inland, bypassing those specific sedimentary-magmatic observations at the Plate margin. As mentioned above, two collisional events in the Late Mesozoic on the southern margin of Eurasia are constrained to 166–157 Ma and 151–129 Ma through intraplate deformation, respectively. Intriguingly and coincidentally, the precise timing of these two inferred collisions corresponds perfectly with those of tectonic events declared in previous studies (Zhu et al., 2016; Ma et al., 2017, 2018; Yang et al., 2017; Hao et al., 2019; Sun et al.,2019; Shi et al., 2020; Zeng et al., 2021, 2022), no matter what exactly the events are, which will be helpful to understand the tectonic evolution of the southern margin of Eurasia.

Studies on intraplate deformation demonstrate that only when full plate coupling is achieved can the stress propagate to the inland and deformation occur (Dickerson, 2003), or a major collisional event at the plate boundary, rather than collisional force generated during subduction is most likely to be responsible for the build-up of significant intraplate compressional stresses (Ziegler et al.,1998; Raimondo et al., 2014). Thus, the tectonic event during 166–157 Ma on the southern margin of Eurasia must have been a collision rather than the subduction and subsequent retardation of the ocean plateau or microcontinent on the BNO (Chen et al., 2018; Yan and Zhang, 2020; Shi et al., 2020). Further, the so-called Lhasa-Qiangtang collision at ca.166 Ma (Ma et al., 2017) cannot explain the disappearance of compressive stress in the Kimmeridgian-Tithonian, corresponding to the deposition of Toutunhe Formation and Qigu Formation in the Junggar Basin, and the re-emergence of greater intraplate compressional stress in Lastest Jurassic-Earliest Cretaceous. Therefore, we prefer that the Karakoram Block initially collided with the South Pamir Block at ca.167 Ma.

Similarly, the tectonic event on the southern margin of Eurasia during 151–129 Ma was definitely a collision. Hypothesis III of the Lhasa-Qiangtang collision mentioned above is based on the premise that the southern Qiangtang remained in oceanic environments during 150–130 Ma. If the in-plane stress during 150 Ma-130 Ma in the Junggar Basin was derived from the proposed oceanic plateau subduction (Hao et al., 2019; Shi et al., 2020), corresponding to the J/K unconformity, then the alleged Lhasa-Qiangtang collision at ca.100–90 Ma must have generated greater compressive stress and more conspicuous stratigraphic records of intraplate deformation in the Junggar Basin, such as extensive unconformity between the Lower and Upper Cretaceous. Unfortunately, despite the absence of the Upper Cretaceous in some areas of the eastern Junggar Basin (Fig. 2e; Wu et al., 2021), a complete sequence of the Upper Cretaceous is developed in the interior of the basin, as well as the southern margin of the basin, with no conformity (Fig. 2c and Fig. 3b; Fang et al., 2015b; Song, 2019; Zhang, 2020; Zhang et al., 2022). Of greater significance, AFT age of ca.80–50 Ma and cooling mainly in ca. 80 Ma (Fig. 7a-b) reveal the exhumation of Chinese Tianshan occurring during Late Cretaceous to Eocene, which does not coincide with Hypothesis III of ca. 100–90 Ma and may be the main cause of upper Cretaceous deficiency in eastern Junggar Basin.

These points, taken together, lead us to conclude that the first period of intraplate deformation in ca.166–157 Ma probably corresponds to the Karakoram-South Pamir collision, while the second intracontinental deformation during ca.151–129 Ma indicates the occurrence of the major collision between Lhasa and Qiangtang terranes.

5. Conclusion

(1) Dating results of syndepositional detrital zircons contain crucial information about coeval intraplate deformation and the precise deformation timing corresponding to unconformities of the late Middle Jurassic and the Lastest Jurassic-Earliest Cretaceous in the Junggar Basin can be constrained to ca.166–157 Ma and 151–129 Ma respectively.

(2) Two periods of intraplate deformation of the Junggar Basin in the Late Mesozoic should be attributed to the tectonic compression of the southern margin of Eurasia, among which, the deformation during 166–157 Ma is probably attributed to the Karakoram-South Pamir collision, while the deformation during 151–129 Ma is proposed to be the produce of Lhasa-Qiangtang collision.

Declaration of Competing Interest.

The authors declare that they have no potential conflict of interest.

CRediT authorship contribution statement

Zhaojian Wu: Conceptualization, Funding acquisition, Methodology, Investigation, Formal analysis, Writing – original draft. **Xiaoyong Yang:** Methodology, Writing – review & editing, Resources, Supervision, Project administration. **Saijun Sun:** Methodology, Writing – review & editing, Resources, Supervision, Project administration. **Jiang Zhu:** Resources, Supervision, Data curation, Validation. **Xiaowen Hu:** Investigation, Software, Validation. **Xiaozhong Han:** Investigation, Validation. **Yifeng Cai:** Investigation, Data curation. **Hui Ji:** Investigation, Data curation.

Declaration of Competing Interest

The authors declare that they have no known competing financial interests or personal relationships that could have appeared to influence the work reported in this paper.

Data availability

Data will be made available on request.

Acknowledgments

This work was financially supported by the National Natural Science Foundation of China (42202088) and the National Key Research and Development Program of China (No. 2018YFC0604204). We are highly grateful to Dr. Yujie Hao of Jilin University for his help in the Zircon U-Pb dating and to the Editorial Office for polishing the full text.

Appendix A. Supplementary data

Supplementary data to this article can be found online at https://doi.org/10.1016/j.jseaes.2023.105755.

References

Aitken, A.R.A., Betts, P.G., Ailleres, L., 2009. The architecture, kinematics, and lithospheric processes of a compressional intraplate orogen occurring under

Gondwana assembly: The Petermann orogeny, central Australia. Lithosphere 1 (6), 343–357.
Andersen, T., 2002. Correction of common lead in U-Pb analyses that do not report ^{204}Pb. Chem. Geol. 192 (1–2), 59–79.
Bian, W., Yang, T., Ma, Y., Jin, J., Gao, F., Zhang, S., Wu, H., Li, H., 2017. New Early Cretaceous palaeomagnetic and geochronological results from the far western Lhasa terrane: Contributions to the Lhasa-Qiangtang collision. Sci. Rep. 7 (1), 1–14.
Bosworth, W., Guiraud, R., Kessler, L.G., 1999a. Late Cretaceous (ca. 84 Ma) compressive deformation of the stable platform of northeast Africa (Egypt): Far-field stress effects of the "Santonian event" and origin of the Syrian arc deformation belt. Geology 27 (7), 633–636.
Bosworth, W., Guiraud, R., Kessler, L.G., 1999b. Late Cretaceous (ca. 84 Ma) compressive deformation of the stable platform of northeast Africa (Egypt): Far-field stress effects of the "Santonian event" and origin of the Syrian arc deformation belt. Geology 27, 633–636.
Buslov, M.M., De Grave, J., Bataleva, E.A.V., Batalev, V.Y., 2007. Cenozoic tectonic and geodynamic evolution of the Kyrgyz Tien Shan Mountains: A review of geological, thermochronological and geophysical data. J. Asian Earth Sci. 29 (2–3), 205–214.
Charvet, J., Shu, L., Laurent-Charvet, S., Wang, B., Faure, M., Cluzel, D., Chen, Y., De Jong, K., 2011. Palaeozoic tectonic evolution of the Tianshan belt, NW China. Sci. China Earth Sci. 54, 166–184.
Chen, Y.F., Ding, L., Li, Z.Y., Laskowski, A.K., Li, J.X., Baral, U., Qasim, M., Yue, Y.H., 2020. Provenance analysis of Cretaceous peripheral foreland basin in central Tibet: Implications to precise timing on the initial Lhasa-Qiangtang collision. Tectonophysics 775, 228311.
Chen, W. Y., Hu, X. C., Zhong, Y., Fu, Y. B., Li, F., Wang, Y. G., 2018. Comment on "Sedimentary and tectonic evolution of the southern Qiangtang basin: Implications for the Lhasa-Qiangtang collision timing" by A. Ma et al. Journal of Geophysical Research: Solid Earth 123(9), 7338-7342.
Chen, C., Lu, H., Jia, D., Cai, D., Wu, S., 1999. Closing history of the southern Tianshan oceanic basin, western China: an oblique collisional orogeny. Tectonophysics 302 (1–2), 23–40.
Chen, X., Shu, L., Santosh, M., Zhao, X., 2013. Island arc-type bimodal magmatism in the eastern Tianshan Belt, Northwest China: Geochemistry, zircon U-Pb geochronology and implications for the Paleozoic crustal evolution in Central Asia. Lithos 168–169, 48–66.
Cloetingh, S., Van Wees, J.D., 2005. Strength reversal in Europe's intraplate lithosphere: Transition from basin inversion to lithospheric folding. Geology 33 (4), 285–288.
Cunningham, D., 2005. Active intracontinental transpressional mountain building in the Mongolian Altai: Defining a new class of orogen. Earth Planet. Sci. Lett. 240 (2), 436–444.
De Grave, J., Buslov, M.M., 2007. Distant effects of India-Eurasia convergence and Mesozoic intracontinental deformation in Central Asia: Constraints from apatite fission-track thermochronology. J. Asian Earth Sci. 29 (2–3), 188–204.
De Grave, J., Buslov, M.M., Van Den Haute, P., Metcalf, J., Dehandschutter, B., McWilliams, M.O., 2009. Multi-method chronometry of the Teletskoye graben and its basement, Siberian Altai Mountains: new insights on its thermo-tectonic evolution. Geol. Soc. Lond. Spec. Publ. 324 (1), 237–259.
De Grave, J., Glorie, S., Buslov, M.M., Izmer, A., Fournier-Carrie, A., Batalev, V.Y., Vanhaecke, F., Elburg, M., Van den haute, P., 2011. The thermo-tectonic history of the Song-Kul plateau, Kyrgyz Tien Shan: Constraints by apatite and titanite thermochronometry and zircon U/Pb dating. Gondw. Res. 20 (4), 745–763.
De Grave, J., De Pelsmaeker, E., Zhimulev, F.I., Glorie, S., Buslov, M.M., 2014. Meso-Cenozoic building of the northern Central Asian Orogenic Belt: Thermotectonic history of the Tuva region. Tectonophysics 621, 44–59.
De Grave, J., Van den haute, P., 2002. Denudation and cooling of the Lake Teletskoye Region in the Altai Mountains (South Siberia) as revealed by apatite fission-track thermochronology. Tectonophysics 349 (1–4), 145–159.
Dickerson, P.W., 2003. Intraplate mountain building in response to continent–continent collision—the Ancestral Rocky Mountains (North America) and inferences drawn from the Tien Shan (Central Asia). Tectonophysics 365 (1–4), 129–142.
Dong, Y., Zhang, G., Neubauer, F., Liu, X., Hauzenberger, C., Zhou, D., Li, W., 2011. Syn- and post-collisional granitoids in the Central Tianshan orogen: geochemistry, geochronology and implications for tectonic evolution. Gondw. Res. 20, 568–581.
Dumitru, T.A., Zhou, D., Chang, E.Z., Graham, S.A., Hendrix, M.S., Sobel, E.R., Carroll, A. R., 2001. Uplift, exhumation, and deformation in the Chinese Tian Shan. Memoirs-Geological Society of America 71–100.
Fang, Y., Wu, C., Guo, Z., Hou, K., Dong, L., Wang, L., Li, L., 2015b. Provenance of the southern Junggar Basin in the Jurassic: Evidence from detrital zircon geochronology and depositional environments. Sed. Geol. 315, 47–63.
Fang, Y., Wu, C., Wang, Y., Hou, K., Guo, Z., 2019. Topographic evolution of the Tianshan Mountains and their relation to the Junggar and Turpan Basins, Central Asia, from the Permian to the Neogene. Gondw. Res. 75, 47–67.
Fang, S., Zhao, M., Zhuo, Q., 2015a. Meso-Cenozoic tectonic and sedimentary evolution of Junggar Basin. Petroleum Industry Press, Beijing, China (in Chinese).
Galbraith, R.F., 2005. Statistics for Fission Track Analysis. CRC Press.
Galbraith, R.F., Laslett, G.M., 1993. Statistical models for mixed fission track ages. Nucl. Tracks Radiat. Meas. 21 (4), 459–470.
Glorie, S., De Grave, J., 2016. Exhuming the Meso-Cenozoic Kyrgyz Tianshan and Siberian Altai-Sayan: a review based on low-temperature thermochronology. Geosci. Front. 7 (2), 155–170.
Glorie, S., De Grave, J., Buslov, M.M., Zhimulev, F.I., Stockli, D.F., Batalev, V.Y., Izmer, A., Van den haute, P., Vanhaecke, F. and Elburg, M.A.,, 2011. Tectonic history of the Kyrgyz South Tien Shan (Atbashi-Inylchek) suture zone: The role of inherited structures during deformation-propagation. Tectonics 30 (6), TC6016.
Glorie, S., Otasevic, A., Gillespie, J., Jepson, G., Danišík, M., Zhimulev, F.I., Gurevich, D., Zhang, Z., Song, D., Xiao, W., 2019. Thermo-tectonic history of the Junggar Alatau within the Central Asian Orogenic Belt (SE Kazakhstan, NW China): Insights from integrated apatite U/Pb, fission track and (U–Th)/He thermochronology. Geosci. Front. 10 (6), 2153–2166.
Graham, S.A., Hendrix, M.S., Johnson, C.L., Badamgarav, D., Badarch, G., Amory, J., Porter, M., Barsbold, R., Webb, L.E., Hacker, B.R., 2001. Sedimentary record and tectonic implications of Mesozoic rifting in southeast Mongolia. Geol. Soc. Am. Bull. 113 (12), 1560–1579.
Han, Y., Zhao, G., 2018. Final amalgamation of the Tianshan and Junggar orogenic collage in the southwestern Central Asian Orogenic Belt: Constraints on the closure of the Paleo-Asian Ocean. Earth Sci. Rev. 186, 129–152.
Hao, L.L., Wang, Q., Zhang, C., Ou, Q., Yang, J.H., Dan, W., Jiang, Z.Q., 2019. Oceanic plateau subduction during closure of the Bangong-Nujiang Tethyan Ocean: Insights from central Tibetan volcanic rocks. GSA Bull. 131 (5–6), 864–880.
Hartmann, L.A., Santos, J.O.S., 2004. Predominance of high Th/U, magmatic zircon in Brazilian Shield sandstones. Geology 32 (1), 73–76.
He, Z., Wang, B., Glorie, S., Su, W., Ni, X., Jepson, G., Liu, J., Zhong, L., Gillespie, J., De Grave, J., 2022. Mesozoic building of the Eastern Tianshan and East Junggar (NW China) revealed by low-temperature thermochronology. Gondw. Res. 103, 37–53.
Hendrix, M.S., Graham, S.A., Carroll, A.R., Sobel, E.R., McKNIGHT, C.L., Schulein, B.J., Wang, Z., 1992. Sedimentary record and climatic implications of recurrent deformation in the Tian Shan: Evidence from Mesozoic strata of the north Tarim, south Junggar, and Turpan basins, northwest China. Geol. Soc. Am. Bull. 104, 53–79.
Jolivet, M., Dominguez, S., Charreau, J., Chen, Y., Li, Y., Wang, Q., 2010. Mesozoic and Cenozoic tectonic history of the central Chinese Tian Shan: Reactivated tectonic structures and active deformation. Tectonics 29 (6), TC6019.
Lai, W., Hu, X., Garzanti, E., Xu, Y., Ma, A., Li, W., 2019. Early Cretaceous sedimentary evolution of the northern Lhasa terrane and the timing of initial Lhasa-Qiangtang collision. Gondw. Res. 73, 136–152.
Leier, A.L., DeCelles, P.G., Kapp, P., Gehrels, G.E., 2007. Lower Cretaceous strata in the Lhasa Terrane, Tibet, with implications for understanding the early tectonic history of the Tibetan Plateau. J. Sediment. Res. 77 (10), 809–825.
Li, S., Guilmette, C., Ding, L., Xu, Q., Fu, J.J., Yue, Y.H., 2017. Provenance of Mesozoic clastic rocks within the Bangong-Nujiang suture zone, central Tibet: Implications for the age of the initial Lhasa-Qiangtang collision. J. Asian Earth Sci. 147, 469–484.
Li, D., He, D., Qi, X., Zhang, N., 2015. How was the Carboniferous Balkhash-West Junggar remnant ocean filled and closed? Insights from the Well Tacan-1 strata in the Tacheng Basin. NW China. Gondwana Research 27 (1), 342–362.
Li, S.M., Wang, Q., Zhu, D.C., Cawood, P.A., Stern, R.J., Weinberg, R., Zhao, Z., Mo, X.X., 2020. Reconciling orogenic drivers for the evolution of the Bangong-Nujiang Tethys during Middle-Late Jurassic. Tectonics 39 (2).
Li, W., 2007. The Mechanic and tectonic evolution of Mesozoic basins in northwestern Junggar orogenic belt. Chinese Academy of Geological Sciences, Beijing, China (in Chinese with English abstract).
Liu, S., Dou, H., Li, H., Wen, Z., 2019a. Geological significance of the discovery of Late Jurassic intermediate-acidic intrusive rock in Bogeda area of East Tianshan, Xinjiang, and its U-Pb zircon age. Geol. Bull. China 38, 288–294 in Chinese with English abstract.
Liu, B., Han, B.F., Chen, J.F., Ren, R., Zheng, B., Wang, Z.Z., Feng, L.X., 2017. Closure Time of the Junggar-Balkhash Ocean: Constraints from Late Paleozoic Volcano-Sedimentary Sequences in the Barleik Mountains, West Junggar. NW China. Tectonics 36 (12), 2823–2845.
Liu, Y., Wang, M., Li, C., Li, S., Xie, C., Zeng, X., Dong, Y., Liu, J., 2019b. Late Cretaceous tectono-magmatic activity in the Nize region, central Tibet: evidence for lithospheric delamination beneath the Qiangtang-Lhasa collision zone. Int. Geol. Rev. 61 (5), 562–583.
Long, X., Wu, B., Sun, M., Yuan, C., Xiao, W., Zuo, R., 2020. Geochronology and geochemistry of Late Carboniferous dykes in the Aqishan-Yamansu belt, eastern Tianshan: Evidence for a post-collisional slab breakoff. Geosci. Front. 11, 347–362.
Luo, A.B., Wang, M., Zeng, X.W., Hao, Y.J., Li, H., 2021. An extensional collapse model for the Lhasa-Qiangtang orogen in Central Tibet. Gondw. Res. 89, 66–87.
Ma, D., He, D., Li, D., Tang, J., Liu, Z., 2015. Kinematics of syn-tectonic unconformities and implications for the tectonic evolution of the Hala'alat Mountains at the northwestern margin of the Junggar Basin, Central Asian Orogenic Belt. Geoscience Frontiers 6 (2), 247–264.
Ma, A., Hu, X., Garzanti, E., Han, Z., Lai, W., 2017. Sedimentary and tectonic evolution of the southern Qiangtang basin: Implications for the Lhasa-Qiangtang collision timing. J. Geophys. Res. Solid Earth 122 (7), 4790–4813.
Ma, Y., Yang, T., Bian, W., Jin, J., Wang, Q., Zhang, S., Wu, H., Li, H., Cao, L., 2018. A stable southern margin of Asia during the Cretaceous: Paleomagnetic constraints on the Lhasa-Qiangtang collision and the maximum width of the Neo-Tethys. Tectonics 37 (10), 3853–3876.
Marshak, S., Karlstrom, K., Timmons, J.M., 2000. Inversion of Proterozoic extensional faults: An explanation for the pattern of Laramide and Ancestral Rockies intracratonic deformation, United States. Geology 28 (8), 735–738.
Morin, J., Jolivet, M., Robin, C., Heilbronn, G., Barrier, L., Bourquin, S., Jia, Y., 2018. Jurassic paleogeography of the Tian Shan: an evolution driven by far-field tectonics and climate. Earth Sci. Rev. 187, 286–313.
Neil, E.A., Houseman, G.A., 1997. Geodynamics of the Tarim Basin and the Tian Shan in central Asia. Tectonics 16 (4), 571–584.
Parizot, O., Missenard, Y., Vergely, P., Haurine, F., Noret, A., Delpech, G., Barbarand, J., Sarda, P., 2020. Tectonic record of deformation in intraplate domains: case study of far-field deformation in the Grands Causses Area, France. Geofluids 2020, 1–19.
Pinet, N., 2016. Far-field effects of Appalachian orogenesis: a view from the craton. Geology 44 (2), 83–86.

Raimondo, T., Hand, M., Collins, W.J., 2014. Compressional intracontinental orogens: Ancient and modern perspectives. Earth Sci. Rev. 130, 128–153.
Roberts, E.A., Houseman, G.A., 2001. Geodynamics of central Australia during the intraplate Alice Springs Orogeny: thin viscous sheet models. Geol. Soc. Lond. Spec. Publ. 184 (1), 139–164.
Shi, L.Z., Huang, J.Y., Chen, W., 2020. Birth and demise of the Bangong-Nujiang Tethyan Ocean: A review from the Gerze area of Central Tibet: Comment. Earth Sci. Rev. 208, 103209.
Song, X., 2019. Sedimentary characteristics of the Upper Cretaceous Donggou formation in the Soutern margin of Junggar Basin. China University of Petroleum, Qingdao, China (in Chinese with English abstract).
Stephenson, R., Schiffer, C., Peace, A., Nielsen, S.B., Jess, S., 2020. Late Cretaceous-Cenozoic basin inversion and palaeostress fields in the North Atlantic-western Alpine-Tethys realm: implications for intraplate tectonics. Earth Sci. Rev. 210, 103252.
Sun, G.Y., Hu, X.M., Zhu, D.C., Hong, W.T., Wang, J.G., Wang, Q., 2015. Thickened juvenile lower crust-derived ~90 Ma adakitic rocks in the central Lhasa terrane. Tibet. Lithos 224, 225–239.
Sun, G., Hu, X., Xu, Y., BouDagher-Fadel, M.K., 2019. Discovery of Middle Jurassic trench deposits in the Bangong-Nujiang suture zone: Implications for the timing of Lhasa-Qiangtang initial collision. Tectonophysics 750, 344–358.
Sun, M., Tang, J.X., Chen, W., Ma, X.D., Qu, X.M., Song, Y., Li, X., Ding, J.S., 2020. Process of lithospheric delamination beneath the Lhasa-Qiangtang collision orogen: Constraints from the geochronology and geochemistry of Late Cretaceous volcanic rocks in the Lhasa terrane, central Tibet. Lithos 356, 105219.
Vermeesch, P., 2012. On the visualisation of detrital age distributions. Chem. Geol. 312, 190–194.
Vermeesch, P., 2018. IsoplotR: A free and open toolbox for geochronology. Geosci. Front. 9 (5), 1479–1493.
Vermeesch, P., 2021. Maximum depositional age estimation revisited. Geosci. Front. 12 (2), 843–850.
Vetrov, E.V., Buslov, M.M., De Grave, J., 2016. Evolution of tectonic events and topography in southeastern Gorny Altai in the Late Mesozoic-Cenozoic (data from apatite fission track thermochronology). Russ. Geol. Geophys. 57 (1), 95–110.
Wang, Z., 2009. Research on the tectonic event and thermal evolution history of piedmont zone in north margin of Junggar Basin. Northwest University, Xi'an, China in Chinese with English abstract.
Wang, S., Gao, L., 2012. SHRIMP U-Pb dating of zircons from tuff of Jurassic Qigu Formation in Junggar Basin, Xinjiang. Geol. Bull. China 31, 503–509 in Chinese with English abstract.
Wang, F., Luo, M., He, Z., Ge, R., Cao, Y., De Grave, J., Zhu, W., 2022a. Late Mesozoic intracontinental deformation and magmatism in the Chinese Tianshan and adjacent areas, Central Asia. Geol. Soc. Am. Bull. 134 (11–12), 3003–3021.
Wang, S., Yang, T., Gao, F., Bian, W., Jin, J., Peng, W., Jiao, X., Ma, J., Zhang, S., Wu, H., Li, H., Cao, L., 2022b. Paleomagnetic and geochronological results of the Risong Formation in the western Lhasa Terrane: Insights into the Lhasa-Qiangtang collision and stratal age. Palaeogeogr. Palaeoclimatol. Palaeoecol. 586, 110778.
Wei, Y., Zhao, Z., Niu, Y., Zhu, D.C., DePaolo, D.J., Jing, T., Liu, D., Guan, Q., Sheikh, L., 2020. Geochemistry, detrital zircon geochronology and Hf isotope of the clastic rocks in southern Tibet: implications for the Jurassic-Cretaceous tectonic evolution of the Lhasa terrane. Gondw. Res. 78, 41–57.
Wiedenbeck, M., Alle, P., Corfu, F., Griffin, W.L., Meier, M., Oberli, F., Vonquadt, A., Roddick, J.C., Spiegel, W., 1995. Three natural zircon standards for U-Th-Pb, Lu-Hf, trace element and REE analyses. Geostand. Newslett. 19 (1), 1–23.
Wu, Z., Han, X., Ji, H., Cai, Y., Xue, L., Sun, S., 2021. Mesozoic-Cenozoic tectonic events of eastern Junggar Basin, NW China and their significance for uranium mineralization: Insights from seismic profiling and AFT dating analysis. Ore Geol. Rev. 139, 104488.
Wu, Y., Zheng, Y., 2004. Genesis of zircon and its constraints on interpretation of U-Pb age. Chin. Sci. Bull. 49, 1554–1569.
Wu, K., Zhong, Y., Yuan, Y., Wan, Z., Xia, B., Wu, T., 2022. Early Cretaceous Granitoids Magmatism in the Nagqu Area, Northern Tibet: Constraints on the Timing of the Lhasa-Qiangtang Collision. Minerals 12 (8), 933.
Xu, W., Ji, W., Song, B., Li, Y., Zhao, Y., Wang, B., Zhang, H., Ye, X., Wei, X., McLachlan, P., 2021. Primary Carboniferous paleomagnetic and geochronologic results from the Aqishan-Yamansu Belt, Eastern Tianshan: Implications for the tectonic evolution of the Paleo-Asian Ocean. Tectonophysics 818, 229070.
Yan, L.L., Zhang, K.J., 2020. Infant intra-oceanic arc magmatism due to initial subduction induced by oceanic plateau accretion: A case study of the Bangong Meso-Tethys, central Tibet, western China. Gondw. Res. 79, 110–124.
Yang, F., 2012. The basement property and evolution of the northern Junggar Basin by in-situ Analysis of zircon U-Pb chronology and trace element. Northwest University, Xi'an, China in Chinese with English abstract.
Yang, Y.T., Guo, Z.X., Luo, Y.J., 2017. Middle-Late Jurassic tectonostratigraphic evolution of Central Asia, implications for the collision of the Karakoram-Lhasa Block with Asia. Earth Sci. Rev. 166, 83–110.
Yang, P., Huang, Q.T., Zhang, K.J., Kapsiotis, A., Zheng, H., Peng, T.P., Zhou, R., Yang, Q., Luo, W., Xia, B., 2022. Compositional signatures of ophiolitic rocks from the Dongco massif: Novel insights into the evolution of the central Tibetan Meso-Tethyan oceanic plateau. Lithos 416, 106660.
Yang, Y.T., Song, C.C., He, S., 2015. Jurassic tectonostratigraphic evolution of the Junggar basin, NW China: A record of Mesozoic intraplate deformation in Central Asia. Tectonics 34 (1), 86–115.
Yi, J.K., Wang, Q., Zhu, D.C., Li, S.M., Liu, S.A., Wang, R., Zhang, L., Zhao, Z.D., 2018. Westward-younging high-Mg adakitic magmatism in central Tibet: Record of a westward-migrating lithospheric foundering beneath the Lhasa-Qiangtang collision zone during the Late Cretaceous. Lithos 316, 92–103.
Yuan, H., Gao, S., Liu, X., Li, H., Günther, D., Wu, F., 2004. Accurate U-Pb age and trace element determinations of zircon by laser ablation-inductively coupled plasma-mass spectrometry. Geostand. Geoanal. Res. 28 (3), 353–370.
Zeng, Y.Y., Sun, C.H., 2022. The timing of the Lhasa-Qiangtang collision revealed from the paleomagnetic age of the Qiangtang Basin, Tibetan Plateau. Appl. Geophys. 1–20.
Zeng, Y.C., Xu, J.F., Chen, J.L., Wang, B.D., Huang, F., Xia, X.P., Li, M.J., 2021. Early Cretaceous (~138-134 Ma) Forearc Ophiolite and Tectonomagmatic Patterns in Central Tibet: Subduction Termination and Re-initiation of Meso-Tethys Ocean Caused by Collision of an Oceanic Plateau at the Continental Margin? Tectonics 40 (3).
Zhang, Y., Liu, S., Liu, Y., Xia, Z., Gao, X., Cha, X., Fan, Y., 2022. Sedimentary Filling Characteristics and Environmental Analysis of Late Cretaceous Donggou Formation in Southern Margin of Junggar Basin, Xinjiang. Geol. 40 (2), 223–229 in Chinese with English abstract.
Zhang, X., Zhao, G., Eizenhöfer, P.R., Sun, M., Han, Y., Hou, W., Liu, D., Wang, B., Liu, Q., Xu, B., 2015. Latest Carboniferous closure of the Junggar Ocean constrained by geochemical and zircon U-Pb–Hf isotopic data of granitic gneisses from the Central Tianshan block, NW China. Lithos 238, 26–36.
Zhang, X., Zhao, G., Sun, M., Eizenhöfer, P.R., Han, Y., Hou, W., Liu, D., Wang, B., Liu, Q., Xu, B., 2016. Tectonic evolution from subduction to arc-continent collision of the Junggar ocean: Constraints from U-Pb dating and Hf isotopes of detrital zircons from the North Tianshan belt, NW China. Geol. Soc. Am. Bull. 128, 644–660.
Zhang, L., 2020. Geological architecture, sedimentary filling, formation and mechanism of the Carboniferous basin in the Junggar area, NW China. China University of Geosciences (Beijing), Beijing, China (in Chinese with English abstract).
Zhao, Z., Bons, P.D., Stübner, K., Wang, G.H., Ehlers, T.A., 2017. Early cretaceous exhumation of the Qiangtang Terrane during collision with the Lhasa Terrane. Central Tibet. Terra Nova 29 (6), 382–391.
Zhu, D.C., Li, S.M., Cawood, P.A., Wang, Q., Zhao, Z.D., Liu, S.A., Wang, L.Q., 2016. Assembly of the Lhasa and Qiangtang terranes in central Tibet by divergent double subduction. Lithos 245, 7–17.
Zhu, W., Wang, R., Lu, X., Shi, W., Ren, M., Liu, K., 2021. Yanshanian tectonic activities and their sedimentary responses in Northwestern Junggar Basin. Earth Sci. 46 (5), 1692–1709 in Chinese with English abstract.
Zhu, Z., Zhai, Q., Hu, P., Tang, Y., Wang, H., Wang, W., Wu, H., 2022. Resolving the timing of Lhasa-Qiangtang block collision: Evidence from the Lower Cretaceous Duoni Formation in the Baingoin foreland basin. Palaeogeogr. Palaeoclimatol. Palaeoecol. 595, 110956.
Ziegler, P.A., Van Wees, J.D., Cloetingh, S., 1998. Mechanical controls on collision-related compressional intraplate deformation. Tectonophysics 300, 103–129.